OPEN

Optimal Contrast of Cerebral Dual-Energy Computed Tomography Angiography in Patients With Spontaneous Subarachnoid Hemorrhage

Dan Wang, MD, Qiaowei Zhang, MD,* Hongjie Hu, MD,* Wenming Zhang, MD,* Renbiao Chen, MD,* Chi S. Zee, MD,† and Risheng Yu, MD‡*

Objective: The aim of this study was to investigate the image quality of cerebral dual-energy computed tomography (CT) angiography using a nonlinear image blending technique as compared with the conventional linear blending method in patients with spontaneous subarachnoid hemorrhage (SAH).

Methods: A retrospective review of 30 consecutive spontaneous SAH patients who underwent a dual-source, dual-energy (80 kV and Sn140 kV mode) cerebral CT angiography was performed with permission from hospital ethical committee. Optimized images using nonlinear blending method were generated and compared with the 0.6 linear blending images by evaluating cerebral artery enhancement, attenuation of SAH, image noise, signal-to-noise ratio (SNR), and contrast-to-noise ratio (CNR), respectively. Two neuroradiologists independently assessed subjective vessel visualization per segment using a 5-point scale.

Results: The nonlinear blending images showed higher cerebral artery enhancement (307.24 ± 58.04 Hounsfield unit [HU]), lower attenuation of SAH (67.07 ± 6.79 HU), and image noise (7.18 ± 1.20 HU), thus achieving better SNR (43.92 ± 11.14) and CNR (34.34 ± 10.25), compared with those of linear blending images (235.47 ± 46.45 HU for cerebral artery enhancement, 70.00 ± 6.41 HU for attenuation of SAH, 8.39 ± 1.25 HU for image noise, 28.86 ± 8.43 for SNR, and 20.37 ± 7.74 for CNR) (all $P < 0.01$). The segmental scorings of the nonlinear blending image (31.6% segments with a score of 5, 57.4% segments with a score of 4, 11% segments with a score of 3) ranged significantly higher than those of linear blending images (11.5% segments with a score of 5, 77.5% segments with a score of 4, 11% segments with a score of 3) ($P < 0.01$). The interobserver agreement was good ($\kappa = 0.762$), and intraobserver agreement was excellent for both observers ($\kappa = 0.844$ and 0.858, respectively).

Conclusions: The nonlinear image blending technique improved vessel visualization of cerebral dual-energy CT angiography by optimizing contrast enhancement in spontaneous SAH patients.

Key Words: nonlinear blending, dual energy, computed tomography angiography, subarachnoid hemorrhage

(*J Comput Assist Tomogr* 2016;40: 48–52)

From the *Department of Radiology, Sir Run Run Shaw Hospital, School of Medicine, Zhejiang University, Zhejiang, China; †Department of Radiology, USC University Hospital, Keck School of Medicine, University of Southern California, Los Angeles, CA; and ‡Department of Radiology, Second Affiliated Hospital of Zhejiang University School of Medicine, Hangzhou, Zhejiang, China.

Received for publication May 16, 2015; accepted September 14, 2015.

Correspondence to: Risheng Yu, MD, Department of Radiology, Second Affiliated Hospital of Zhejiang University School of Medicine, 88 Jiefang Rd, Hangzhou, Zhejiang 310009, China (e-mail: cjr.yurisheng@vip.163.com).

The authors declare no conflict of interest.

DOI: 10.1097/RCT.0000000000000336

Spontaneous subarachnoid hemorrhage (SAH), approximately 80% caused by the rupture of intracranial aneurysms, is a devastating disorder with an extremely poor prognosis.[1] Computed tomography (CT) angiography (CTA) is commonly used as the first-line diagnostic modality in detecting intracranial aneurysm due to its noninvasive nature and the cost efficiency.[2] In clinical practice, however, cerebral CTA in patients with massive spontaneous SAH could sometimes be presented with unsatisfactory image quality due to poor intracranial artery contrast, owing to the high-density hemorrhage in basal cisterns and poor contrast agent filling of the intracranial artery caused by decreased cerebral perfusion secondary to vasospasm and intracranial hypertension.[1,3–5]

Dual-energy CT angiography is known to provide improved contrast resolution over conventional CTA by blending 2 energy data sets into a single mixed image set.[6,7] The postprocessing approach used for image blending can be a linear or nonlinear technique.[8] The latter has been demonstrated with superior image contrast in several previous studies working on detection of hypervascular pathologies or abdominal vessel visualization.[9–13]

The purpose of our study was to investigate how the nonlinear blending method ameliorated the image quality of cerebral DECTA compared with the linear blending method in spontaneous SAH patients.

MATERIALS AND METHODS

Patients

Three hundred ninety-three patients had cerebral DECTA in our department from February 2014 to July 2013. A total of 35 consecutive patients presented with massive spontaneous SAH suspected for intracranial aneurysms were retrospectively evaluated. Three patients with intracranial metal artifacts and 2 patients with inadequate data sets were excluded. Thirty patients were finally enrolled in this study. The group of patients was consisted of 12 men and 18 women, with a mean age of 61.73 years ranging from 28 to 80 years. The study was approved by the institutional review board of our hospital.

CT Examination

All of the patients were scanned on a second-generation dual-source CT system (Definition Flash; Siemens AG, Forchheim, Germany). All cerebral CTA were performed using dual-source, dual-energy mode, with the tube voltage and current 80 kVp/Sn140 kVp and 177 mA/89 mA, respectively. The other parameters used included the following: 2 × 128 × 0.6 mm acquisition collimation by using flying focus spot; gantry rotation time, 0.28 second; pitch, 0.7; 0.75-mm slice thickness; and 0.5-mm slice distance with 250-mm scan field of view and a medium soft convolution kernel of D10f. The caudal-cranial direction was used for all imaging.

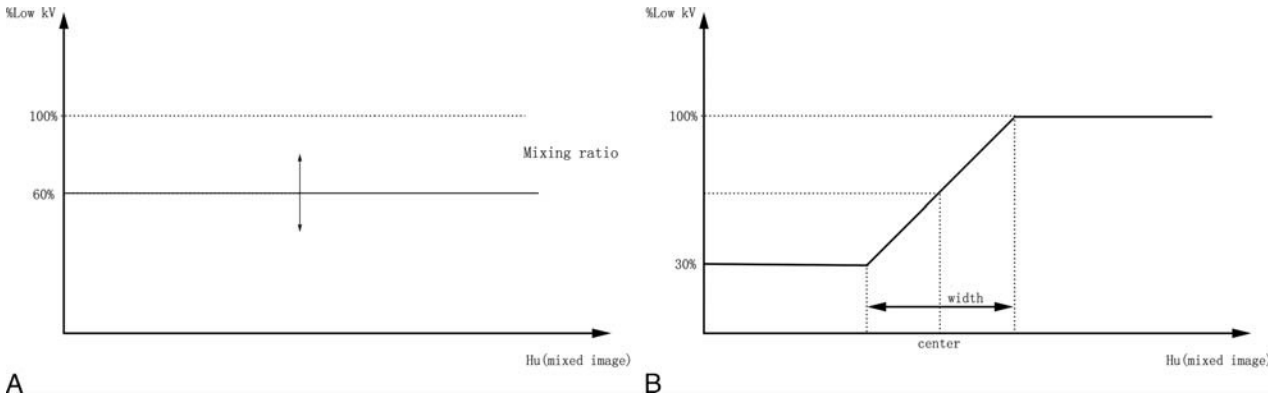

FIGURE 1. Illustration of the linear (A) and nonlinear (B) image blending technique in DECTA. In linear blending method, the 2 energy data sets were blended with a fixed ratio (0.6) for each pixel independent of the voxel CT value. In nonlinear blending method (a modified sigmoid function referred to as moidal blending function), however, the mixing ratio of each pixel was calculated according to its attenuation value and adjusted by the 2 parameters BC and BW. Pixels with CT values less than BC-BW/2 in the linearly blended reference images were shifted toward a blending ratio of 0.3 for a minimized noise; pixels with CT value greater than the BC + BW/2 were shifted toward a 100% weight of low kV data sets for a maximized contrast; pixels with CT value within the range of BW were blended with a variable ratio increased linearly as demonstrated by the oblique line.

The contrast agent (350 mg iodine/mL, Iohexol; Beilu Pharma, Beijing, China) was intravenously injected through antecubital vein via 20-gauge needle by a power injector (SCT-210; Medrad Inc, Indianola, Pa). A total amount of 40 mL contrast agent, followed by 40 mL saline solution at flow rates of 4 mL/s, was used for all patients. The scan delay was individually determined by a bolus-tracking technique with trigger threshold set at 100 Hounsfield unit (HU) on the ascending aorta.

All images were transferred to a workstation (MMWP; Siemens AG, Forchheim, Germany) for image evaluation. After DECTA acquisition, the linear mixing image sets were reconstructed automatically using a ratio of 0.6 (0.6 80 kVp + 0.4 140 kVp). The optimized images using nonlinear image blending method were reconstructed based on a modified sigmoid function (Fig. 1), which was referred to as "optimum contrast" in the commercial software supplied within the workstation. The blending center and blending width were set around 100 to 150 HU and 20 to 30 Hounsfield unit (HU), respectively, in the nonlinear image blending process.

The CT volume dose index and the dose-length product were automatically determined and recorded from the CT scanner at the end of each examination. The mean CT volume dose index and dose-length product for the DECTA were 6.53 ± 0.23 mGy and 120 ± 11.67 mGy · cm, respectively.

Assessment of Image Quality

The quantitative image quality was evaluated by cerebral artery enhancement, attenuation of SAH, image noise, and the following calculated signal-to-noise ratio (SNR) and contrast-to-noise ratio (CNR). For each patient, the attenuation values of the proximal segment (M1) of middle cerebral arteries (MCAs) (which was defined as the cerebral artery enhancement) and the surrounding SAH were measured at the same slice and same location of the 2 image sequences. The regions of interest (ROI) was maintained as large as possible with vessel wall and calcifications and/or soft plaques avoided. The image noise was defined as the standard deviation of the attenuation value measured in vitreous with ROI as larger as possible (Fig. 2). The contrast was the difference of CT value between M1 and SAH. Signal-to-noise ratio was calculated as the attenuation values of M1 divided by image noise, and CNR was the contrast divided by image noise.

All of the images were evaluated independently by 2 neuroradiologists who were blinded to patient history and the blending

FIGURE 2. Example of quantitative image quality measurement. The ROI was placed at the M1 segment of MCA (A) and the surrounding SAH (B). The image noise was defined as the standard deviation of the attenuation value measured in vitreous with ROI as larger as possible (C).

TABLE 1. Quantitative Measurement of Image Quality

Blending Method	M1, HU	SAH, HU	Noise, HU	SNR	CNR
Nonlinear	307.24 ± 58.04	67.07 ± 6.79	7.18 ± 1.20	43.92 ± 11.14	34.34 ± 10.25
Linear	235.47 ± 46.45	70.00 ± 6.41	8.39 ± 1.25	28.86 ± 8.43	20.37 ± 7.74
P-value			<0.001 for all parameters		

M1 indicates segment of middle cerebral artery.

methods. The maximum intensity projection images were used for evaluation on a commercial workstation (MMWP). When there was a discrepancy between 2 readers, a joint-reading session was used to reach consensus. Cerebral arteries were rated per segment on a 5-point scale: 5, excellent, no obvious image noise and artifacts, sharp vessel structures, and satisfactory details; 4, good, mild image noise and artifacts, less clear vessel structures and details; 3, fair, moderate image noise and artifacts, optimal enhancement but insufficient for diagnosis; 2, poor, severe image noise and artifacts, suboptimal vessel, inadequate for diagnosis; 1, undiagnosable, severe image noise and artifacts, blurry vessel structures, no diagnosis possible. The segments surrounding the circle of Willis, including bilateral middle cerebral artery (M1, M2), anterior cerebral artery (A1, A2), posterior cerebral artery (P1, P2), anterior communicating artery, and posterior communicating artery, were evaluated, respectively.

Statistical Analysis

The statistical analysis was performed using SPSS (SPSS version 15; SPSS Inc, Chicago, Ill). The paired Student *t* test was used to compare the CT values of the intracranial artery and the background SAH, image noise, SNR, and CNR between the linear and nonlinear blending images. The Wilcoxon–Mann-Whitney tests were used to estimate the segmental scorings of the 2 image sequences. The interobserver and intraobserver agreement was calculated by κ test (κ < 0.2, slight or poor agreement; 0.2–0.4, fair agreement; 0.4–0.6, moderate agreement; 0.6–0.8, substantial agreement; >0.8, excellent agreement).[14] A *P* value of 0.05 was considered as statistically significant.

RESULTS

Objective Image Analysis

The results of quantitative measurement of image quality were shown in Table 1. The mean attenuation measured in M1 segment was significantly higher in the nonlinearly blended images than the linearly blended images, with a dramatic increase of 72 HU ($P < 0.01$). However, the mean CT value of background SAH and the image noise were significantly lower in the nonlinearly blended images compared with those of linearly blended images, although the differences were slight (both $P < 0.01$). Because of the increased cerebral artery enhancement and the decreased attenuation of SAH and image noise, the calculated SNR and CNR of the nonlinearly blended images were also significantly superior compared with those of linearly blended images, with an improvement of 15.06 and 13.97, respectively (both $P < 0.01$).

Subjective Image Analysis

Table 2 displayed the results of qualitative evaluation of image quality for each group on a per-segment–based analysis. A total of 383 segments were present and evaluated. None of the evaluated segments were ranked as poor or undiagnosable. The segmental scorings of the nonlinear blending image (31.6% segments with a score of 5, 57.4% segments with a score of 4, 11% segments with a score of 3) ranged significantly higher than those of linear blending images (11.5% segments with a score of 5, 77.5% segments with a score of 4, 11% segments with a score of 3) ($P < 0.01$) (Fig. 3). The interobserver agreement was good (κ = 0.762). Intraobserver agreement between the first and second evaluation of image quality for both observers reached excellent agreement with κ statistics of 0.844 and 0.858, respectively.

DISCUSSION

Inadequate intracranial artery contrast might be primarily responsible for the unsatisfactory image quality of cerebral CTA in patients with massive spontaneous SAH. Generally, multiple strategies can be applied for the purpose of increasing vascular opacification during the examination of CTA, such as elevating the amount, concentration or injection flow rate of contrast media,[15–17] or lowing the tube voltage[18] in single energy scan. In DECTA, with both low-energy and high-energy data sets available, vessel visualization can be improved in another way by using blended images. Theoretically, low-kilovolt scan provides images with better iodine contrast at the price of higher noise, whereas the high-kilovolt images are lower in contrast but less noisy. The standard linear blending technique, which is default set in the second generation of dual-source dual-energy CT system, mixes the 2 energy (80 kV and Sn140 kV) data sets with a fixed ratio for each pixel independent of the voxel CT value. This method allows to produce images to be more than 80 kV or 140 kV like by adjusting the weighting factors but still suboptimal in terms of contrast because the advantages of each data set (contrast or sharpness) are partially offset by its drawbacks (blurring or noise) due to the linear nature of the technique.[8] By contrast, the nonlinear blending method based on the moidal blending function is designed to shift the high-density pixel toward a

TABLE 2. Qualitative Evaluation of Image Quality

Blending Method	Score 5	Score 4	Score 3	Score 2	Score 1	Total
Nonlinear	121 (31.6%)	220 (57.4%)	42 (11%)	0 (0%)	0 (0%)	383
Linear	44 (11.5%)	297 (77.4%)	42 (11%)	0 (0%)	0 (0%)	383

Number in parenthesis shows the percentage of segments with the score in evaluated segments in the group ($P < 0.001$).

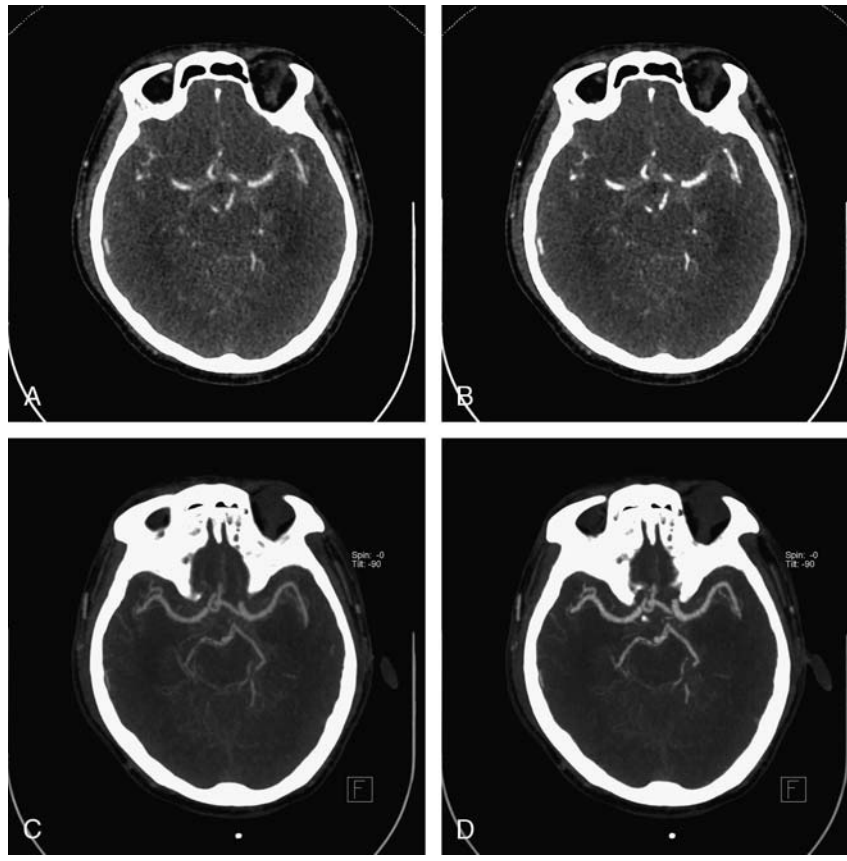

FIGURE 3. Example images from a 50-year-old male patient with sudden headache who received cerebral DECTA after massive SAH was found in the basal cistern. Axial images of the 2 blending method was presented with the same window width (286 HU) and window level (100 HU), showing the difference of CNR between them. CT values of the M1, SAH, and image noise were 188.3 HU, 75.1 HU, and 7.1 HU for linear blending image (A), and 243.4 HU, 70.1 HU, and 5 HU for nonlinear blending image (B), respectively. Two maximum intensity projection images were also presented with the same window width (461 HU) and window level (208 HU), the nonlinear blending image (D) showed obviously brighter intracranial arteries with more clear margin and lower background attenuation and image noise, as compared with the linear blending image (C).

higher weight of 80 kV for maximized iodine contrast and the low-density pixel toward a higher weight of 140 kV for lower background attenuation and noise characteristic (Fig. 1).[8] Taking variable mixing ratio calculated pixel by pixel according to its attenuation value would balance the advantages and disadvantages of both scan mode, thus acquiring optimized image CNR.

The present study evaluated the outcome of linear and nonlinear blending in image quality of cerebral DECTA in spontaneous SAH patients. It depicted a prominent improvement (13.97 and 15.06, respectively) of CNR and SNR in nonlinear blending images due to the dramatic increase (approximately 72 HU) in intracranial arterial enhancement in addition to a slight decrease in the image noise and attenuation of background SAH compared with that of linear blending images. Subjectively, more (additional 20%) cerebral arterial segments got a scoring of excellent in nonlinear blending images. Our study definitely confirmed the advantage of nonlinear blending technique in improving vessel visualization by optimizing image contrast resolution. Without altering the routine scan protocol, this postprocessing technique can be easily implemented with the existing data sets.

Early in 2008, initial studies by Eusemann et al[8] and Holmes et al[19] first demonstrated that nonlinear blending of dual-energy data outperformed the linear blending data with improved CNR and visual preference for a variety of different organs and pathologies of interest. After that, DECTA using nonlinear blending function has been experimented for many clinical applications, such as improving the detection of hypervascular liver hepatocellular carcinoma during the arterial phase scan[9] and providing images with better tumor conspicuity in the evaluation of renal masses during the nephrographic phase of enhancement.[10] In a study in pigs by Kartje et al,[11] the delayed myocardial enhancement in acute myocardial infarction (MI) was revealed with enhanced visualization due to the nonlinear image blending in the late-phase DECTA imaging of MI. Similarly, better image quality with optimal contrast and improved vascular visualization in DECTA for portal venography[12] and abdominal angiography[13] has also been presented in 2 recent studies. Our study investigated its application in cerebral CTA in SAH patients and achieved quite satisfactory results with improved vascular visualization. Our results offered a preferred method to analyze image data of cerebral DECTA and encouraged broad postprocessing implementation not only for the goal of easier and faster bone removal[20] but also for the purpose of increasing contrast and better vascular visualization.

A practical problem during the postprocessing of optimum contrast was how to choose the BC and BW values because different combinations of the 2 defining parameters could generate a large number of images with different features. Although optimized

setting of BC and BW was deemed to be organ, pathologies of interest, and patient dependent, there were still some basic principles and guidance that could be followed according to experiences gained from previous studies. For BC, a value taking the average (or at least between the) CT value of the high-contrast region and the low-contrast background should be chosen.[9,11,12] The results of our study were consistent with this suggestion, where the settings were close to the mean difference between the CT values of MCA and the surrounding SAH measured from the linearly blended images. The adjustment of BW was used to provide a sharper or smoother transition between the 2 data sets. A narrow value setting could lead to images with high contrast but might appear artificial sometimes due to abrupt transition between the 2 data sets, while too wide a setting of BW would reduce the degree of contrast. In regard to CTA, a relatively narrow width might be recommended for the purpose of increasing contrast.[12] In the present study, we chose 20 to 30 HU as the BW and achieved an increase in CT values of MCA from 235 HU to 307 HU. Although parameters selected in our study were not necessarily the best optimal value, our study had shown that nonlinear blending images with properly selected parameters indeed provided significant improvement in CNR over images with linear blending method.

We acknowledge the following limitations. First, the study did not comprise a large number of patients but were sufficient to show the advantage of nonlinear blending technique. Second, not all segments of the intracranial arteries were evaluated, for the reason that majority of the intracranial aneurysms were located adjacent to the circle of Willis.[21] Third, diagnostic performance of each blending method was not assessed for detection and evaluation of aneurysms. This was intended to be a preliminary study to evaluate the feasibility of using nonlinear blending technique for assessing intracranial vessels. A large scale prospective study to assess this technique for the evaluation of intracranial aneurysms is being planned.

In conclusion, our study indicated the nonlinear image blending technique was superior to the linear blending technique in vascular visualization for cerebral DECTA by optimizing contrast enhancement in spontaneous SAH patients. This optimum contrast function of DECTA can be pursued with a broader range of clinical applications in the future.

REFERENCES

1. Suarez JI, Tarr RW, Selman WR. Aneurysmal subarachnoid hemorrhage. *N Engl J Med*. 2006;354:387–396.
2. Sailer AM, Grutters JP, Wildberger JE, et al. Cost-effectiveness of CTA, MRA and DSA in patients with non-traumatic subarachnoid haemorrhage. *Insights Imaging*. 2013;4:499–507.
3. Zhang H, Zhang B, Li S, et al. Whole brain CT perfusion combined with CT angiography in patients with subarachnoid hemorrhage and cerebral vasospasm. *Clin Neurol Neurosurg*. 2013;115:2496–2501.
4. Sanelli PC, Jou A, Gold R, et al. Using CT perfusion during the early baseline period in aneurysmal subarachnoid hemorrhage to assess for development of vasospasm. *Neuroradiology*. 2011;53:425–434.
5. Honda M, Sase S, Yokota K, et al. Early cerebral circulatory disturbance in patients suffering subarachnoid hemorrhage prior to the delayed cerebral vasospasm stage: xenon computed tomography and perfusion computed tomography study. *Neurol Med Chir*. 2012;52:488–494.
6. Vlahos I, Chung R, Nair A, et al. Dual-energy CT: vascular applications. *AJR Am J Roentgenol*. 2012;199:S87–S97.
7. Behrendt FF, Schmidt B, Plumhans C, et al. Image fusion in dual energy computed tomography: effect on contrast enhancement, signal-to-noise ratio and image quality in computed tomography angiography. *Invest Radiol*. 2009;44:1–6.
8. Eusemann C, Holmes DR 3rd, Schmidt B, et al. Dual energy CT: how to best blend both energies in one fused image? *SPIE*. 2008;6918: 691803–691808.
9. Kim KS, Lee JM, Kim SH, et al. Image fusion in dual energy computed tomography for detection of hypervascular liver hepatocellular carcinoma: phantom and preliminary studies. *Invest Radiol*. 2010;45:145–157.
10. Ascenti G, Krauss B, Mazziotti S, et al. Dual-energy computed tomography (DECT) in renal masses: nonlinear versus linear blending. *Acad Radiol*. 2012;19:1186–1193.
11. Kartje JK, Schmidt B, Bruners P, et al. Dual energy CT with nonlinear image blending improves visualization of delayed myocardial contrast enhancement in acute myocardial infarction. *Invest Radiol*. 2013;48:41–45.
12. Wang Q, Shi G, Liu X, et al. Optimal contrast of computed tomography portal venography using dual-energy computed tomography. *J Comput Assist Tomogr*. 2013;37:142–148.
13. Lv P, Liu J, Wu R, et al. Use of non-linear image blending with dual-energy CT improves vascular visualization in abdominal angiography. *Clin Radiol*. 2014;69:e93–e99.
14. Landis JR, Koch GG. The measurement of observer agreement for categorical data. *Biometrics*. 1977;33:159–174.
15. Fujikawa A, Tsuchiya K, Imai M, et al. CT angiography covering both cervical and cerebral arteries using high iodine concentration contrast material with dose reduction on a 16 multidetector-row system. *Neuroradiology*. 2010;52:291–295.
16. Meyer BC, Klein S, Krix M, et al. Comparison of a standard and a high-concentration contrast medium protocol for MDCT angiography of the lower limb arteries. *Rofo*. 2012;184:527–534.
17. Schoellnast H, Deutschmann HA, Berghold A, et al. MDCT angiography of the pulmonary arteries: influence of body weight, body mass index, and scan length on arterial enhancement at different iodine flow rates. *AJR Am J Roentgenol*. 2006;187:1074–1078.
18. Beitzke D, Wolf F, Edelhauser G, et al. Computed tomography angiography of the carotid arteries at low kV settings: a prospective randomised trial assessing radiation dose and diagnostic confidence. *Eur Radiol*. 2011;21: 2434–2444.
19. Holmes DR 3rd, Fletcher JG, Apel A, et al. Evaluation of non-linear blending in dual-energy computed tomography. *Eur J Radiol*. 2008;68: 409–413.
20. Postma AA, Hofman PA, Stadler AA, et al. Dual-energy CT of the brain and intracranial vessels. *AJR Am J Roentgenol*. 2012;199:S26–S33.
21. Forget TR Jr, Benitez R, Veznedaroglu E, et al. A review of size and location of ruptured intracranial aneurysms. *Neurosurgery*. 2001;49: 1322–1325; discussion 1325–1326.